Design and Control of an Anthropometric Robotic Leg

S.Guccione G.Muscato G.Spampinato

Abstract— **This paper describes the theoretical design and the physical realization of an anthropometric robotic leg. It contains a brief description of the mechanical structure as well as the hardware and software architecture. The aim of this project is the development of new technologies for the implementation and realization of bio-mechanical limb for motoric gait rehabilitation. Moreover the work presented describes the implementation of a control architectures in order to ensure the right stability condition, based on the main gait parameters measurements. For this reason a biaxial inclinometer and a foot pressure sensor have been specifically designed.**

Keywords— **Centre of mass, Prototype model, Control strategy, ZMP.**

I. INTRODUCTION

THE interest of the scientist community in studying biped locomotion is increased in the last decades for many reasons. First of all, the high level of mobility, and the high number of degrees of freedom allows this kind of mobile robot to adapt and move upon very unstructured sloped terrain. Moreover, the study of the walking cycle in biped robot allows the researchers to understand more accurately the strategy actuated by human beings in keeping balance in order to maintain a proper stability level during the gait.

II. BASIC CONCEPTS

In order to develop a theoretical strategy to perform the correct joint trajectories synthesis that ensure a dynamically stable walking gait [1], it is necessary to take into account some basic concepts.

During the walk, two different situations arise in sequence: the statically stable double-support phase in which the whole structure of the robot is supported on both feet simultaneously, and the statically unstable single-support phase when only one foot of the robot is in contact with the ground, while the other foot is being transferred from the back to front position. Thus, during a single walking cycle, the kinematic structure of locomotion changes from an open to a closed kinematic chain.

The biped robot stability, and the foot behaviour in particular, cannot be controlled directly, but in an indirect way, by analysing appropriate dynamics of the overall context; in other words the links acceleration context and the ground reaction force context have to be taken into account. According to this point of view, researchers consider two overall indicator of the biped locomotion stability: the ZMP (Zero Moment Point) notion, and the COP (Centre Of Pressure) notion [2].
The first one is defined as follow:

Theorem 1: ZMP is the point on the walking ground surface at which the horizontal components of the resultant moment generated by active forces and moments acting on humanoid links are equal to zero.

Suppose that the ground applies a pure force to the biped robot at a location point, in order to support the robot in the case of possible overturns; this point is called ZMP.

In the Fig.1 a simplified planar model of the ZMP is shown. Suppose that the whole mass of the robot, indicated by the M letter, is concentrated on the centre of gravity; According with the previous definition, the ZMP can be derived from the relations:

$$M(\ddot{r} - g) \times (\ddot{r} - P) = 0 \quad \text{and} \quad \begin{cases} b = r - P \\ F = M(\ddot{r} - g) \end{cases} \tag{1}$$

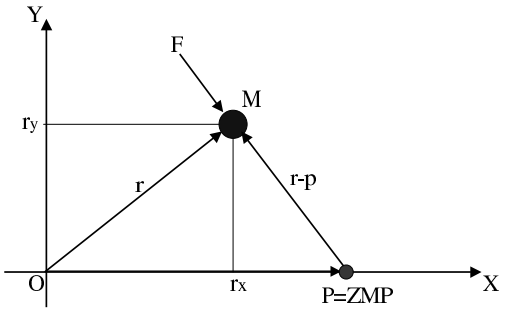

Fig. 1. Simplified planar scheme of the ZMP

in which the F vector represents the force acting to the M point, and the b segment represents the arm of the torque acting to the P point developed by the F force.

Applyng the vector product definition to the (1) relation, the parallelism condition between the F segment and the *(r-p)* segment can be derived.

$$| M(\ddot{r} - g) | \cdot | (\ddot{r} - P) | \cdot | sin(\theta) | = 0 \tag{2}$$

Indeed the relation (2) is satisfied any time only if $sen(\theta)=1 \; \forall \; \theta$.

Giovanni Muscato: Dipartimento di Ingegneria Elettrica Elettronica e dei Sistemi Viale A. Doria 6 95125 CATANIA ITALY Tel: +39-095-7382321 FAX: +39-095-330793 e-mail: gmuscato@dees.unict.it.

Posing the third component of the vector product equal to zero, the x-coordinate of the ZMP can be derived:

$$M(\ddot{r}_y - g) \cdot (\ddot{r}_x - P) - M\ddot{r}_x r_y = 0$$
$$P = \frac{M(\ddot{r}_y - g) \cdot r_x - M\ddot{r}_x r_y}{M(\ddot{r}_y - g)} \tag{3}$$

Generalizing the previous theory to an m centers of mass system:

$$P = \frac{\sum_i^m M_i(\ddot{r}_{yi} - g) \cdot r_{xi} - \sum_i^m M_i \ddot{r}_{xi} r_{yi}}{\sum_i^m M_i(\ddot{r}_{yi} - g)} \tag{4}$$

In order to maintain the necessary stability during the walking cycle, the following condition has to be achieved:

Theorem 2: The gait is balanced when and only when the ZMP trajectory remains within the support area.

In which the support area represents the convex polygon whose vertexes are the robot contact points with the ground.
In this way the system dynamics is perfectly balanced by ground reaction force, and the ZMP trajectory coincides with COP (Centre of pressure) trajectory inside the contact surface.
The COP is defined as follow:

Theorem 3: COP represents the point on the support foot polygon at which the resultant of distributed foot ground reaction forces acts.

Moreover, during the walking cycle, the COP position moves from the hill to the toe of the sole. In this way, the biped locomotion mechanism acquires stability and speed in the movements.

III. PROTOTYPE MODELS

A kinematical model of the whole prototype structure was made using two different points of view. In the first case a three-dimensional model of the prototype is developed, while in the second case, a planar model restriction to the sagittal plane is found in order to minimize the control algorithm computational load, and minimize the simulations time.

A. 3D Model

According with the well known Denavit-Hartenberg rules [3], the prototype kinematical model is developed, and shown in the Fig.2. As it is possible to see, four reference frames are considered:

Σ_0 : The global reference frame.
Σ_1 : The foot reference frame.
Σ_2 : The shinbone reference frame.
Σ_3 : The thighbone reference frame.

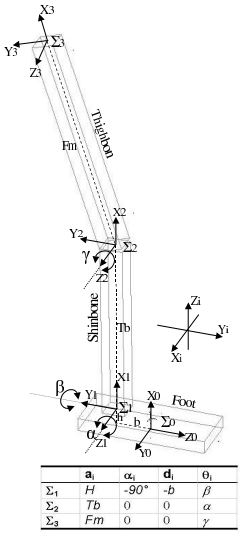

	a_i	α_i	d_i	θ_i
Σ_1	H	-90°	-b	β
Σ_2	Tb	0	0	α
Σ_3	Fm	0	0	γ

Fig. 2. Prototype kinematical model and the corresponding Denavit-Hartenberg parameters

Using the $P_i \equiv (x_i y_i z_i)$ notation to represents the centre of gravity of the i-link, having each of them a corresponding mass indicated by the m_i symbol, it is possible to deduce the three spatial coordinates of the prototype global centre of gravity, as shown by the equations:

$$X_{COG} = \frac{x_1 m_1 + x_2 m_2 + x_3 m_3}{m_1 + m_2 + m_3}$$
$$Y_{COG} = \frac{y_1 m_1 + y_2 m_2 + y_3 m_3}{m_1 + m_2 + m_3} \tag{5}$$
$$Z_{COG} = \frac{z_1 m_1 + z_2 m_2 + z_3 m_3}{m_1 + m_2 + m_3}$$

in which P_i coordinates are obtained by the relations:

$$P_1 = T_1^0 \begin{bmatrix} 0 \\ 0 \\ -\frac{b}{2} \end{bmatrix} P_2 = T_1^0 T_2^1 \begin{bmatrix} 0 \\ 0 \\ -\frac{T_b}{2} \end{bmatrix}$$
$$P_3 = T_1^0 T_2^1 T_3^2 \begin{bmatrix} 0 \\ 0 \\ -\frac{F_m}{2} \end{bmatrix} \tag{6}$$

The T_i^j symbol represents the rototranslation matrix that transforms the Σ_i reference frame coordinates into Σ_j reference frame coordinates.
In the same way it is possible to deduce the ZMP coordinates using the following relations [4]:

$$ZMP_X = \frac{\sum_i^3 m_i(\ddot{z}_i - g) \cdot x_i - \sum_i^3 m_i \ddot{x}_i z_i}{\sum_i^3 m_i(\ddot{z}_i - g)}$$
$$ZMP_Y = \frac{\sum_i^3 m_i(\ddot{z}_i - g) \cdot x_i - \sum_i^3 m_i \ddot{x}_i z_i}{\sum_i^3 m_i(\ddot{z}_i - g)} \tag{7}$$

B. 2D Model

As said before, another way to deduce the prototype model is available. Indeed, in this case, a sagittal plane

restriction of the dynamic behaviour is made. To implements the dynamic model of the prototype a three link planar manipulator is considered as shown in the Fig.3; Each link of the manipulator represents a leg segment, and the ground-foot rotation joint is not actuated. As a result of this strategy, an underactuated manipulator is used to approximately reproduce the prototype behaviour; on the other hand, the simulator computational work is easier.

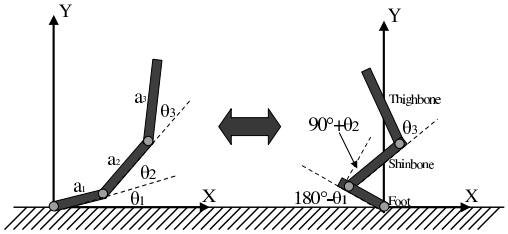

Fig. 3. Three links planar manipulator

As done for the previous approach, the centre of gravity and the ZMP are deduced in a similar way, whereas in this case the centres of mass coordinates have to be derived as shown by the relations:

$$P_1 \equiv \begin{cases} x_1 = l_1 c_1 \\ \\ y_1 = l_1 s_1 \end{cases} \quad P_2 \equiv \begin{cases} x_2 = a_1 c_1 + l_2 c_{12} \\ \\ y_2 = a_1 s_1 + l_2 s_{12} \end{cases}$$
$$P_3 \equiv \begin{cases} x_3 = a_1 c_1 + a_2 c_{12} + l_3 c_{123} \\ \\ y_3 = a_1 s_1 + a_2 s_{12} + l_3 s_{123} \end{cases} \tag{8}$$

Moreover, implementing at the same time the dynamics of an equivalent inverse pendulum, it is possible to deduce the position of COP under the sole [5]; In particular, a typical posture control action is shown in the Fig.4, where the inverse pendulum is indicated by the vertical line connecting the ankle joint with the robot centre of gravity.

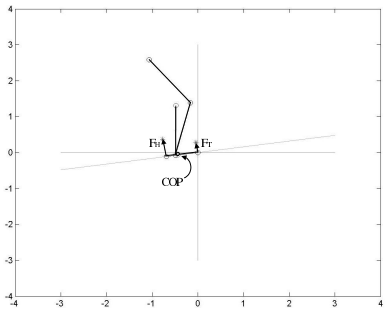

Fig. 4. Prototype planar simulation

In this case, the ground reaction force acting on the toe and heel of the foot are shown, indicated respectively by the F_t and F_h symbols. They can be obtain from the relations (9), depending on the torque t acting on the basis of the pendulum [5],

$$F_t = -\frac{1}{L_t+L_h}\tau + m_t g + frac L_h L_t + L_h f_y$$
$$F_h = -\frac{1}{L_t+L_h}\tau + m_h g + frac L_t L_t + L_h f_y \tag{9}$$

where:

$$m_t = -\frac{L_h+L_G}{L_t+L_h} m \qquad m_h = -\frac{L_t-L_G}{L_t+L_h} m$$
$$F_y = -ML\ddot{\vartheta} sin\vartheta - ML\dot{\vartheta} cos\vartheta + Mg \tag{10}$$

in which L_h and L_t represent respectively the heel and the toe distance from the ankle articulation. Moreover the angular position, velocity, and acceleration, are obtained inverting the relations describing the robot centre of gravity, shown by the relations (11), , that coincides with the superior extremity of the pendulum.

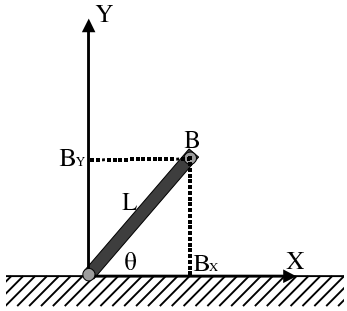

Fig. 5. Centre of mass coordinates

$$\begin{cases} B_X = Lcos\vartheta \\ \\ B_Y = Lsin\vartheta \end{cases} \begin{cases} \dot{B}_X = -Lsin\vartheta\dot{\vartheta} \\ \\ \dot{B}_Y = Lcos\vartheta\dot{\vartheta} \end{cases}$$
$$\begin{cases} \ddot{B}_X = -L(cos\vartheta\dot{\vartheta}^2 + sin\vartheta\ddot{\vartheta}) \\ \\ \ddot{B}_Y = L(sin\vartheta\dot{\vartheta}^2 + cos\vartheta\ddot{\vartheta}) \end{cases} \tag{11}$$

Finally, the base torque τ is obtained from the classical pendulum dynamics relation:

$$I\ddot{\vartheta} = MLsin\vartheta + \tau \qquad I = ML^2 \tag{12}$$

Once F_t and F_h values during the simulation are known, a proportional relation can be used to derive COP position:

$$(F_t - F_h) : x = (F_{max} - F_{min}) : \frac{L_t+L_h}{2}$$
$$x = \frac{(F_t-F_h)}{(F_{max}-F_{min})} \frac{(L_t+L_h)}{2} \tag{13}$$

Just by definition, COP cannot be outside the foot contact surface, so the value derived has to be opportunely saturated.

IV. CONTROL STRATEGIES

In order to test different control strategies, a typical destabilizing situation is created. Indeed a two degrees of freedom sloping platform is made, so the robot, that stands on it, see the ground surface to tilt into roll and pitch direction with respect to the horizontal plane. In the Fig.6 the overall structure is shown.

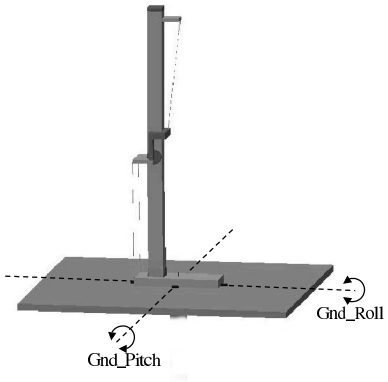

Fig. 6. 3D Prototype simulation

It is important to note that the kinematical model parameters, derived in the previous section, have to be recalculated considering the effect of the sloping ground surface described by the matrix:

$$M = \begin{bmatrix} 1 & 0 & 0 & 0 \\ 0 & cosp & -sinp & 0 \\ 0 & sinp & cosp & 0 \\ 0 & 0 & 0 & 1 \end{bmatrix} \begin{bmatrix} cosr & 0 & -sinr & 0 \\ 0 & 1 & 0 & 0 \\ sinr & 0 & cosr & 0 \\ 0 & 0 & 0 & 1 \end{bmatrix} \quad (14)$$

In order to maintain a right stability margin, it is very useful to measure the ground slope, in both degrees of freedom. To do this a biaxial inclinometer has to be used; supposing to place it on the thighbone superior extremity, some useful relations can be derived from the Fig.7.

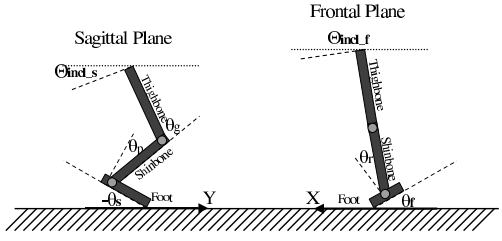

Fig. 7. Inclinometer angular position scheme

In this case the ground slope can be obtained depending on the other joint angular positions; In particular:
For the sagittal plane:

$$\vartheta_s = -(\tilde{\vartheta} - \vartheta_{incl_s}) \quad \text{where} \quad \tilde{\vartheta} = -\vartheta_p + \vartheta_g \quad (15)$$

For the frontal plane:

$$\vartheta_f = -(\tilde{\vartheta} - \vartheta_{incl_f}) \quad \text{where} \quad \tilde{\vartheta} = -\vartheta_r \quad (16)$$

Only using these information it is possible to control the robot stability acting on the ankle joint, in order to compensate the ground slopes. Moreover it is possible to improve the control performance introducing a proportional action based on the robot centre of gravity position, that provides a further contribution that is added to the inclinometer measures. Maximum angular variation range is shown in the Fig.8.

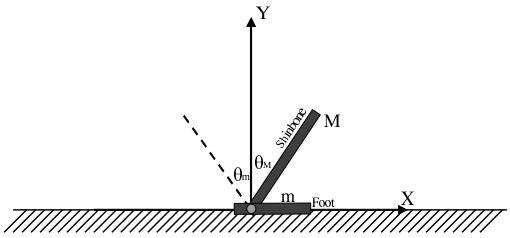

Fig. 8. Ankle proportional action

Formulating a proportional relation between control angular action and the controlled variable error:

$$(\delta_{Max} - \delta_{min}) : \delta = (\vartheta_{Max} - \vartheta_{min}) : (x - \vartheta_0) \quad (17)$$

$$x = \frac{\delta(\vartheta_{Max} - \vartheta_{min})}{(\delta_{max} - \delta_{min})} + \vartheta_0$$

If the x-coordinate centre of gravity error is considered, the relations (18) have to be adopted, otherwise, if the ground reaction force difference is considered the relations (19) have to be adopted (directly related to COP):

$$\begin{cases} \delta_{Max} = L_t \\ \\ \delta_{min} = -L_h \end{cases} \quad (18)$$

$$\begin{cases} \delta_{Max} = (F_{tMax} - F_{hmin}) \\ \\ \delta_{min} = (F_{tmin} - F_{hMax}) \end{cases} \quad (19)$$

Providing a sinusoidal trajectory movement to the ground surface, both control strategies are actuated, and the results are shown in the Fig.9.

In this case a sinusoidal wave with twenty degrees amplitude was applied in both pitch and roll directions.
In the control strategy discussed up to now, only the ankle joint has been used to ensure the adapted stability margin, maintaining fixed the knee joint; but there are some cases in which the knee movement is necessary. Suppose that the centre of gravity height has to be lowered, fixing the ground plane to the horizontal position; in this case, if a forward ankle joint movement acts, a corresponding backward knee joint movement has to be developed, in order to maintain the x-coordinate centre of gravity within the

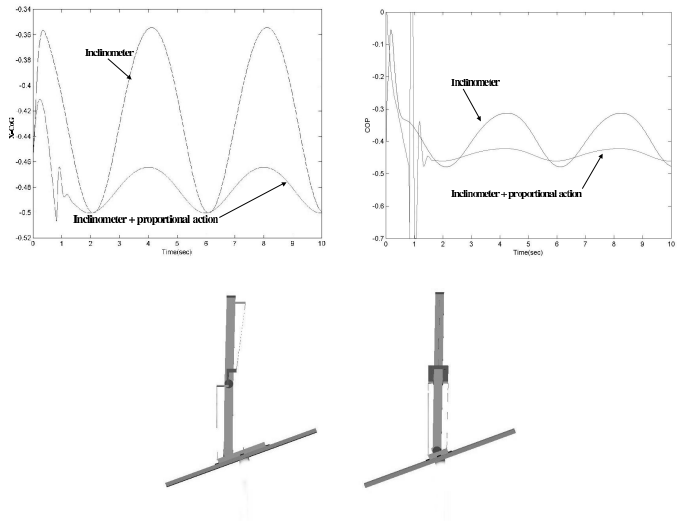

Fig. 9. Simulations results

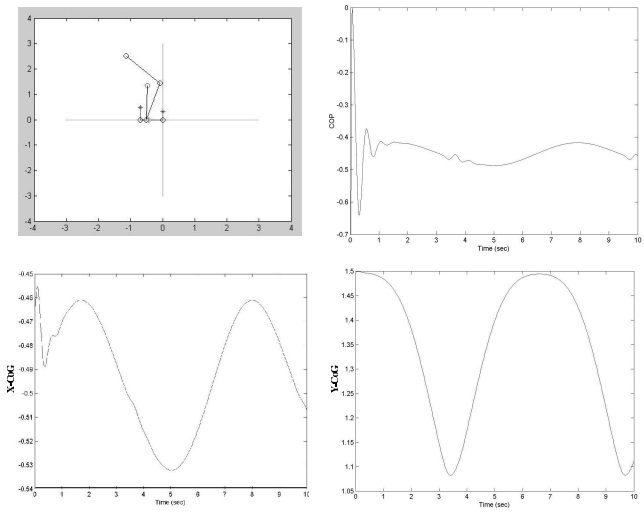

Fig. 10. Simulations results

foot-ground contact surface. To do this, it is possible to reformulate the (5) and (6) relations as follow:

$$\begin{cases} (m_1 l_1 + m_2 a_1 + m_3 a_1) cos\vartheta_1 + (m_2 l_2 + m_3 a_2) cos(\vartheta_1 + \vartheta_2) + \dots \\ \qquad \dots + m_3 l_3 cos(\vartheta_1 + \vartheta_2 \vartheta_3) = \tilde{B}_x (m_1 + m_2 + m_3) \\ (m_1 l_1 + m_2 a_1 + m_3 a_1) sin\vartheta_1 + (m_2 l_2 + m_3 a_2) sin(\vartheta_1 + \vartheta_2) + \dots \\ \qquad \dots + m_3 l_3 sin(\vartheta_1 + \vartheta_2 \vartheta_3) = \tilde{B}_y (m_1 + m_2 + m_3) \end{cases} \tag{20}$$

where $\tilde{B}_x$ and $\tilde{B}_y$ represents the desired x and y centre of gravity coordinates; resolving the first equation with respect of q3 angle:

$$\vartheta_3 = arccos \left[\begin{array}{l} \frac{\tilde{B}_x (m_1+m_2+m_3) - (m_1 l_1 + m_2 a_1 + m_3 a_1)}{m_3 l_3} + \dots \\ \qquad \dots + \frac{-(m_2 l_2 + m_3 a_2) cos(\vartheta_1 + \vartheta_2)}{m_3 l_3} \end{array} \right] - \vartheta_2 - \vartheta_3 \tag{21}$$

that represents the knee angular position that assure the desired $\tilde{B}_x$ value depending on the ground pitch slope position, and the ankle position.
Supposing to unbalance the robot acting the ankle joint by a sinusoidal wave, the knee joint restores the right stability using the (21) relation control strategies as shown in the Fig.10.

V. MECHANICAL STRUCTURE

The design of the shape and the dimensions of the parts that compose the robotic prototype are human inspired, so that the dimensions of the links as well as the articulation movements, are similar to the corresponding biological ones [6]. The mechanical structure of the robotic inferior limb is made up of three links corresponding to femur, tibia and foot, jointed by three degrees of freedom actuated by three pneumatic pistons; In particular the knee joint has one rotational degree of freedom, while the ankle joint has two rotational degrees of freedom. In the Fig.11 a photograph of the prototype is shown:

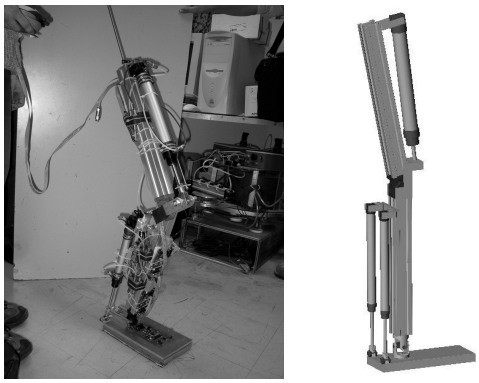

Fig. 11. The prototype realized

As it is possible to see, the whole structure is very compact and reflects the typical anthropometric mass distribution that increases motions stability, as shown by human gait stability theory [7].

VI. CONTROL ARCHITECTURE

In order to control the overall robot structure stability, and to provide the right joint trajectories, a well-constructed control architecture is needed. A complete set of sensors and actuators are placed onboard the robot, and connected to the global control system by a powerful communication system.
The global control algorithm runs inside a PC that represents the system supervisor. The other architecture blocks are shown in the Fig.12.

As discussed in the previous section, a biaxial inclinometer is placed upon the superior extremity of the thighbone bar, and is necessary to implement the right control algorithm. Indeed, this device provides the prototype with the global sense of inclination with respect to the horizontal plane, in both the roll and pitch degrees of freedom.

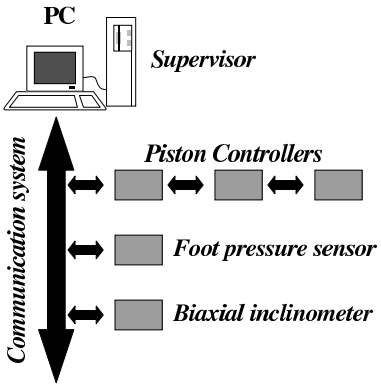

Fig. 12. Control architecture scheme

To pilot the three pneumatic pistons there are three distinct electronic boards, each one realizing a single joint control; indeed each of them pilots only one pneumatic piston, and implements a position control loop inside the card.The control strategy implemented inside the microcontroller is based on the fuzzy theory. Indeed many fuzzy rules are implemented in order to realize a PID controller. The core of each card is a microcontroller unit (MCU) that, appropriately programmed, implements many different control strategies [8].
Finally The prototype is equipped with a foot pressure sensor that measures and localizes the force interacting between sole and ground. Using these informations it is possible to estimate the position of the centre of pressure inside the foot.

VII. PRELIMINARY RESULTS AND CONCLUSIONS

In order to guarantee the whole prototype structure stability, a global control algorithm is implemented inside the PC. Following the control strategies discussed in the previous sections a complete effective control strategy is been implementing and testing. Up to now some useful functionalities are implemented, supported by graphical interfaces, like COP monitoring and articulation trajectory generation. An example of articulation trajectory generation is shown in the Fig.13, where a single walking cycle is reproduced. The knee and ankle trajectories are shown in the Fig.14 in which the sequence numbers 1-2-3 indicate the *Swing Phase*, and the sequence numbers 4-5-6 indicate the *Single Support Phase*. In particular the stage 4, in which it is supposed that the *Double Support Phase* occurs, connects the two phases.

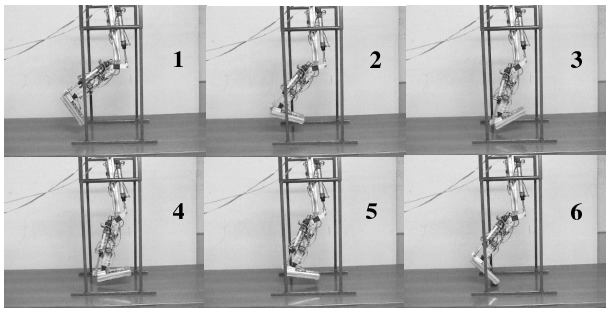

Fig. 13. Walking cycle pattern

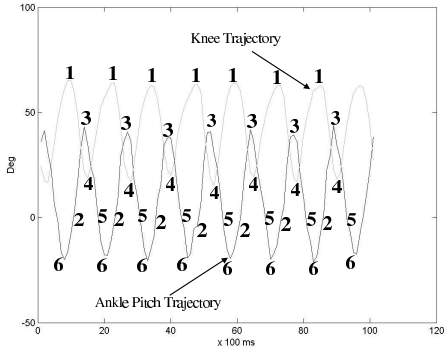

Fig. 14. Knee and ankle trajectories in the walking cycle pattern

References

[1] S. Marchese, G. Muscato, G.S. Virk, *Dynamically stable trajectory synthesis for a biped robot during the single support phase*, Proceedings of the 2001 IEEE/ASME International Conference on Advanced Intelligent Mechatronics, pp. 953-958,Como, Italy July 2001.

[2] Vukobratovic M., Borovac B., Surdilovic D., *Zero Moment Point Proper Interpretation and New Applications*, Fraunhofer Institute IPK-Berlin, Germany. IEEE-RAS International Conference on Humanoid Robots Nov 22-24, 2001 Waseda International Conference Center, Tokyo.

[3] Sciavicco Siciliano, *Modeling and Control of Robot Manipulators*, McGraw-Hill, 1996.

[4] Jong H. Park, Yong K.Rhee, *ZMP Trajectory Generation or Reducerd Trunk motions of Biped Robots*, Conference on Intelligent Robot and Systems, Victoria B.C. Canada, October 1998. Proceeding of the 1998 IEEE/RSJ Intl. Comference on Intelligent Robots and Systems Victoria, B.C., Canada October 1998.

[5] Satoshi Ito, Tomohiro Nishigaki, Haruhisa Kawasaki , *Upright Posture Stabilization by Groung Reaction Force*, Faculty of Engineering, Gifu Univercity, Yanagido 1-1, Gifu 501-1193, Japan.2000, Proceedings of the 2000 IEEE/RSJ International Conference on Intelligent Robots and Systems.

[6] Sardain P., Rostami M., Bessonnet G., *An anthropomorphic biped robot: dynamic concepts and technological design*, IEEE Trans. Syst., Man, Cybern., part A: Systems and Humans, pp. 823-838, vol. 28, No. 6, November, 1998.

[7] Tomomichi Sugihara, Yoshihiko Nakamura, Hirochika Inoue, *Realtime Humanoid Motion Generation through ZMP Manipulation based on Inverted Pendulum Control*, Dep. of Mechano-Informatics, Univ. Of Tokyo, Proceedings of the 2002 IEEE Internatinal Conference on Robotics & Automation Washington DC May 2002.

[8] S. Chillari, S. Guccione and G. Muscato, *An Experimental Comparison Between Several Pneumatic Position Control Methods*, 40th IEEE Conference on Decision and Control, Orlando, USA, Dec. 2001.